The Mystery of Dispersionless Injection of
Energetic Particles Associated With Magnetospheric Substorms

Xinlin Li and D. N. Baker (LASP, University of Colorado, Boulder)
M. Temerin (Space Sciences Lab., University of California, Berkeley)
G. D. Reeves and R. D. Belian (Los Alamos National Lab., Los Alamos, New Mexico)

Ever since Akasofu in 1964 showed that auroral phenomena could be organized into characteristic recurrent patterns called "auroral substorms", people have been arguing the causes of substorms. Lately the debate has centered on the first few minutes of the substorm expansion phase, the so-called "substorm onset". The idea is that the first sign of substorm activity should be located close to the causative source. Two classes of theories, each associated with a different initial location of substorm onset have been promoted: one contends [e.g., Lui, 1996] that substorms start relatively close to the Earth (near the location of geosynchronous orbit at 6.6 Earth radii distant where coincidentally there are a lot of data) or perhaps just a little beyond this geocentric distance. Theories in this class suggest that the electric current that flows in space to produce the Earth's comet-like magnetotail is somehow disrupted close to the Earth. The disruption then propagates further out into the magnetotail where it initiates increased magnetic "reconnection" . During reconnection, "open" magnetic field lines that are connected to the Earth but extend into the solar wind connect to form so-called "closed" magnetic field lines, which are then tied to the Earth at both ends, one end to the northern hemisphere and the other to the southern hemisphere. The other class of theories argues [e.g., Baker et al., 1996] that it is the initiation of or the increase in reconnection at a distance of 20-30 Earth radii, R_E, that begins the substorm expansion phase. It would seem an easy problem to resolve this issue, but because of the sparsity of satellite measurements and because of the fast but nonuniform propagation of signals through the magnetosphere that has not proven to be the case. Our recent simulation results give support to the idea that the initial substorm disturbance originates farther out (>18 R_E) in the magnetotail and then propagates inward as described in the

second of the above mentioned class of substorm theories.

One of the characteristic features of substorm onset is the "dispersionless" particle injection. Here we describe some recent results using test particle simulations of dispersionless injections that are helping to determine the origin of substorms and which also show how dispersionless injections can, in principle, be produced. The term "dispersionless injection" refers to the sudden appearance of energetic ions and electrons over a broad range of energies (tens to hundreds of keV) in the Earth's magnetosphere. Such injection events are often seen near midnight on satellites in geosynchronous orbit in association with substorm onset. Normally dispersion (dispersion in this context means the observation of different energies at different times in analogy to the dispersion of light by a prism which causes different wavelengths to appear at different positions) is caused by the simple fact that more energetic particles move faster than less energetic particles. Thus, if the acceleration of particles occurs somewhere other than the observation point, one would expect dispersion as the more energetic particles reach the satellite sooner. This dispersionless feature of substorm injections has been a long-standing mystery since it did not appear that the particles could all be accelerated locally yet they appeared together in tight, coherent bunches.

Thus it has been assumed that electrons and ions in dispersionless injections must come from nearby. If this were not so, there should be dispersion since the gradient-B drift motion of charged particles is energy dependent. This led to the view that there is a spatial boundary separating different particle distributions. When this boundary crosses the spacecraft, the spacecraft would suddenly see a new population of particles. McIlwain [1974] proposed such an "injection boundary" model of dispersionless injections. The injection boundary model suggests that during the injection a spatial boundary is formed that separates energized plasma from the pre-existing plasma.

Our recent test particle simulations [Li et al., 1998] have shown how dispersionless injections of energetic particles can be produced in association with magnetospheric substorms. Based on our simulation results, we conclude that (1) The source of energetic particles in dispersionless injections at geosynchronous orbit is mostly from more than a few R_E

tailward of geosynchronous orbit indicating that substorms are, as expected, a large scale magnetospheric phenomena. Particles which originate within one to two R_E closer (within one to two R_E from geosynchronous orbit) make a much smaller contribution but produce the initial enhancement. (2) There is no sharp spatial boundary in the initial particle distribution as has sometimes been supposed to explain the dispersionless injection. The dispersionless injection is simply the consequence of an electric field and a self-consistent magnetic field that propagates through the plasma, convecting the plasma inward.

Observations

The left column of Figure 1 is an example of a dispersionless injection measured by the Los Alamos National Laboratory (LANL) sensors on three satellites in geosynchronous orbit. The injected electrons detected by spacecraft 1 (1990-095) appear dispersionless. Later as these electrons drifted around the Earth because of the gradient of the Earth's magnetic field, they are detected by spacecraft 2 (1991-080), but now with dispersion as more energetic electrons arrive earlier. Even later, spacecraft 3 (1994-084) sees them with even more dispersion. These electrons continued to drift completely around the Earth and were detected by the three spacecraft again as periodic flux peaks. These periodic features are called "drift echoes".

Other measurements from geosynchronous satellites separated in local time show that dispersionless injections occur in a fairly narrow region near midnight while measurements from satellites located near the same local time but at different radial distances show that injections occur first at larger radial distances [Reeves et al., 1996]. Dispersionless injections are usually accompanied by rapid reorganizations of the magnetic field as the nightside magnetospheric field becomes more like a dipole field. This is called a "dipolarization" and is one of the central features of substorms.

Modeling

T. Moore et al. [1981] proposed an "injection front" model in which an injection corresponds to a compressional wave front that propagates earthward from a disturbance occurring in the magnetotail. Later attempts to reproduce substorm injection features using the injection front model resulted in too little energization. Therefore it was assumed that some initial energization of the source population was required prior to the dipolarization of the magnetic field and the injection of particles into geosynchronous orbit. For many years magnetic reconnection was considered to be the most likely candidate [e.g., Baker et al., 1996]. Subsequent work showed that the reconnection region was typically located more than 25 R_E down tail–nearly 20 R_E from where the injections were observed. In the last two years the numerical MHD simulations of Birn et al. [e.g., 1998] have helped resolve this apparent contradiction. They found that, although the reconnection region was located quite far from the Earth, the strongest electric fields formed much closer to the Earth and were associated with very fast convective flows known as bursty bulk flows [e.g., Angelopoulos et al., 1994]. The electric fields in the bursty bulk flows help to energize and transport electrons and ions close to geosynchronous orbit and the MHD simulations were able to reproduce many of the observed substorm injection signatures. They did not, however, explain the propagation of substorm injections to geosynchronous orbit where the magnetic field is more dipole-like and bursty bulk flows are not observed.

Using the above ideas of how electric and magnetic fields might change during substorms, we recently investigated dispersionless injections by tracing particles in a constructed model of electric and magnetic fields [Li et al., 1998] and as shown in right column of Figure 1 reproduced quite well the measured particle injection. Our model fields are similar to the ones in Li et al. [1993], which were developed to model the sudden compression of the magnetosphere by a strong interplanetary shock on March 24, 1991. The magnetosonic wave that propagated through the magnetosphere as a consequence of this shock injected ions and electrons with energies larger than 15 MeV in as close to the Earth as $2R_E$ creating a new radiation belt, the most energetic particle injection ever seen in the magnetosphere.

When simulating that event, we learned that an electromagnetic pulse propagating inward could create a dispersionless injection. To model a substorm injection we used a similar field model except that we made the electromagnetic pulse slower, weaker, more confined in local time, and had it originate in the magnetotail rather than in interplanetary space, then we traced test particles in this field model.

Test particle simulations can be used to determine the effect of assumed electric and magnetic fields on given particle distributions. The effects of of magnetic and electric fields on individual particle trajectories are well known and by using test particle simulations one can combine many such trajectories to determine the effects of such fields on particle distributions, which is what is measured by particle detectors on satellites. However, the result is not unique. It is possible for a different field model together with a different initial particle model to give the same results at a given point (but not likely to produce the same results at multiple points). Thus judgment needs to be used to assess how reasonable these models are. We try to use simple models with a minimum of free parameters in trying to reproduce the data.

In our simulation we assumed that the initial energy spectrum of the electrons could be described by a kappa distribution, a low-energy thermal distribution with an additional high-energy tail as is often measured [Christon et al., 1991]. We also assume a simple radial dependence of the intensity of that distribution.

The fields were assumed to be a superposition of a background, nearly dipole, magnetic field and a time-varying electric and magnetic field. The time-varying fields in our model can be associated with the dipolarization process: During dipolarization the northward magnetic field in the equatorial plane increases in association with a temporally and spatially varying electric field pointing predominantly westward. In our model these perturbed fields propagate from the magnetotail toward the Earth at a speed of 100 km/s. The electric field is modeled as a time-dependent Gaussian pulse with a purely azimuthal electric field component that propagates radially inward at a constant velocity and decreases away from midnight. The modeled magnetic field dipolarization occurs first at midnight and subse-

quently at other local times. The time varying magnetic field is obtained from Faraday's law.

The left column of Figure 2 shows observations for protons from the LANL sensors on two satellites at geosynchronous orbit (no proton data are available for spacecraft 1) while the right column shows our simulation results.

To compare with data, we also simulated the detectors' response and orbital motion. In our test particle simulation we followed over half a million electrons and protons as they drifted in the combined pulse and background fields and recorded their energy and arrival time at various local times. The dispersionless feature (as observed for electrons), the drift echo, the double-peak feature (a dip within the first enhancement), even the width and shape of the fluxes are well reproduced for electrons (Figure 1) and for protons as well.

To explain how dispersionless injections are produced in more detail, Figure 3 shows the trajectories and the time history of the radial distance and kinetic energy of two electrons with different initial radial distances, energies, and local times. Before the arrival of the wave field, the electrons only perform a gradient-B drift, whose velocity is energy-dependent. When the wave arrives, marked by the vertical dash-dot line in Figure 3(b), the electrons encounter an oppositely-directed magnetic field gradient due to the wave field, which can reduce or even reverse the local magnetic field gradient, such that the electrons can drift in the opposite direction (westward). Meanwhile, each electron also moves radially inward because of the $\mathbf{E} \times \mathbf{B}$ drift ($V_{\mathbf{E}\times\mathbf{B}} = \mathbf{E} \times \mathbf{B}/\mathrm{B}^2$), which is energy independent. As the electrons move closer to the Earth, the gradient drift of the electron in the background magnetic field begins to dominate the motion and the electron again drifts eastward. After the wave field passes, marked by the vertical dotted line, the electrons again gradient-B drift but in the stronger magnetic field closer to the Earth.

Whether or not dispersion is seen in the initial rise of the particle flux depends on whether the incoming pulse or the gradient drift dominates the changes in the particle flux. At midnight the pulse moves particles of all energy inward simultaneously and thus no dispersion is seen in the initial rise of the particle flux. At other local times the higher

energy particles already affected by the pulse at midnight may arrive before the pulse itself or the pulse may be weak away from midnight. In this case the gradient drift will dominate and dispersion will be seen in the initial arrival of particles of different energy. The same considerations apply to ions except that energetic ions drift westward in the opposite direction.

In order to determine the initial radial location of the particles that contribute to the injected flux, we divided the initial distribution and followed only the particles with initial radial distances greater than 9 R_E. We found that such particles produced more than 90% of the enhancement seen at geosynchronous orbit. The observed injected electrons and protons at geosynchronous orbit come originally from a continuous spatial region: Mostly from a region more than a few R_E away but a smaller portion originate within a couple of R_E as well. Since we have achieved good agreement with data without invoking an injection boundary model, these results suggest that the "injection boundary" is really the consequence of transient electric and magnetic acting on smoothly varying particle distributions.

In summary, dispersionless injections and the onset of substorms can be understood as a consequence of of transient electric and magnetic fields propagating towards the Earth from the magnetotail. When a particle encounters these propagating fields, its motion is dominated by the transient magnetic and electric fields and is directed toward the Earth. Betatron acceleration by the transient fields then leads to energization. While our model of the transient fields is simple, it likely represents the features responsible for the energization and transport of the electrons and ions and it also implicitly contains much of the phenomenology often mentioned in the description of substorm onset [Li et al., 1998].

Figure Caption

Figure 1: Differential fluxes of electrons from LANL observations in the early Jan. 10, 1997 in the left column: number 1, 2, and 3 correspond to spacecraft 1990-095 (LT=UT-2:30), 1991-080 (LT=UT+4:42), and 1994-084 (LT=UT+6:54) respectively. The simulation results are shown in the right column.

Figure 2: Same as Figure 1 but for protons.

Figure 3: (a) trajectory of two electrons with 90° pitch angle initially placed in the equatorial plane with $r_0 = 12R_E$, $W_0 = 26$ keV, and $\phi_0 = 120°$ (red) and $r_0 = 14R_E$, $W_0 = 25$ keV, and $\phi_0 = 135°$ (green). The dotted circle represents r=6.6 R_E. (b) time history of radial distance (solid curves) and kinetic energy (dashed curves) of the two electrons.

REFERENCES CITED

Angelopoulos, V., C. F. Kennel, F. V. Coroniti, R. Pellat, M. G., Kivelson, R. J. Walker, C. T. Russell, W. Baumjohann, W. C. Feldman, and J. T. Gosling, Statistical Characteristics of bursty bulk flow events, *J. Geophys. Res.*, *99*, 21257, 1994.

Baker, D. N., T. I. Pulkkinen, V. Angelopoulos, W. Baumjohann, and R. L. McPherron, Neutral line model of substorms: Past results and present view, *J. Geophys. Res.*, *101*, 12975, 1996.

Birn, J., M. F. Thomsen, J. E. Borovsky, G. D. Reeves, D. J. McComas, R. D. Belian, and M. Hesse, Substorm electron injections: Geosynchronous observations and test particle simulations, *J. Geophys. Res.103*, 9235, 1998.

Christon, S. P., D. J. Williams, and D. G. Mitchell, Spectral characteristics of plasma sheet ion and electron populations during disturbed geomagnetic conditions, *J. Geophys. Res.*, *96*, 1, 1991.

Li, X., D. N. Baker, M. Temerin, G. Reeves, R. Belian, Simulation of Dispersionless Injections and Drift Echoes of Energetic Electrons Associated with Substorms, *Geophys. Res. Lett.25*, 3763, 1998.

Li, X., I. Roth, M. Temerin, J. Wygant, M. K. Hudson, and J. B. Blake, Simulation of the prompt energization and transport of radiation particles during the March 23, 1991 SSC, *Geophys. Res. Lett.20*, 2423, 1993.

Lui, A. T. Y., Current disruption in the Earth's magnetosphere: Observations and models, *J. Geophys. Res.101*, 13067, 1996.

McIlwain, C. E., Substorm injection boundaries, *Magnetospheric Physics*, edited by B. M. McCormac, p. 143, D. Reidel, Hingham, Mass., 1974.

Moore, T. E., R. Arnoldy, J. Feynmann, and D. A. Hardy, Propagating substorm injection fronts, *J. Geophys. Res.86*, 6713, 1981.

Reeves, G. D., R. W. H. Friedel, M. G. Henderson, A. Korth, P. S. McLachlan, and R. D. Belian, Radial propagation of substorm injections, International Conference on Substorms-3, *ESA SP-339*, 579-584, 1996.

For more information, contact Xinlin Li, LASP, CB 590, U. of Colorado, 1234 Innovation Drive, Boulder, CO 80309-0590, E-mail: lix@lasp.colorado.edu Tel: 303-492-3514, Fax: 303-492-6444.

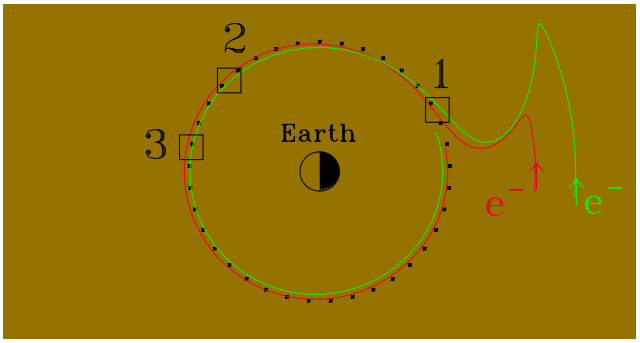

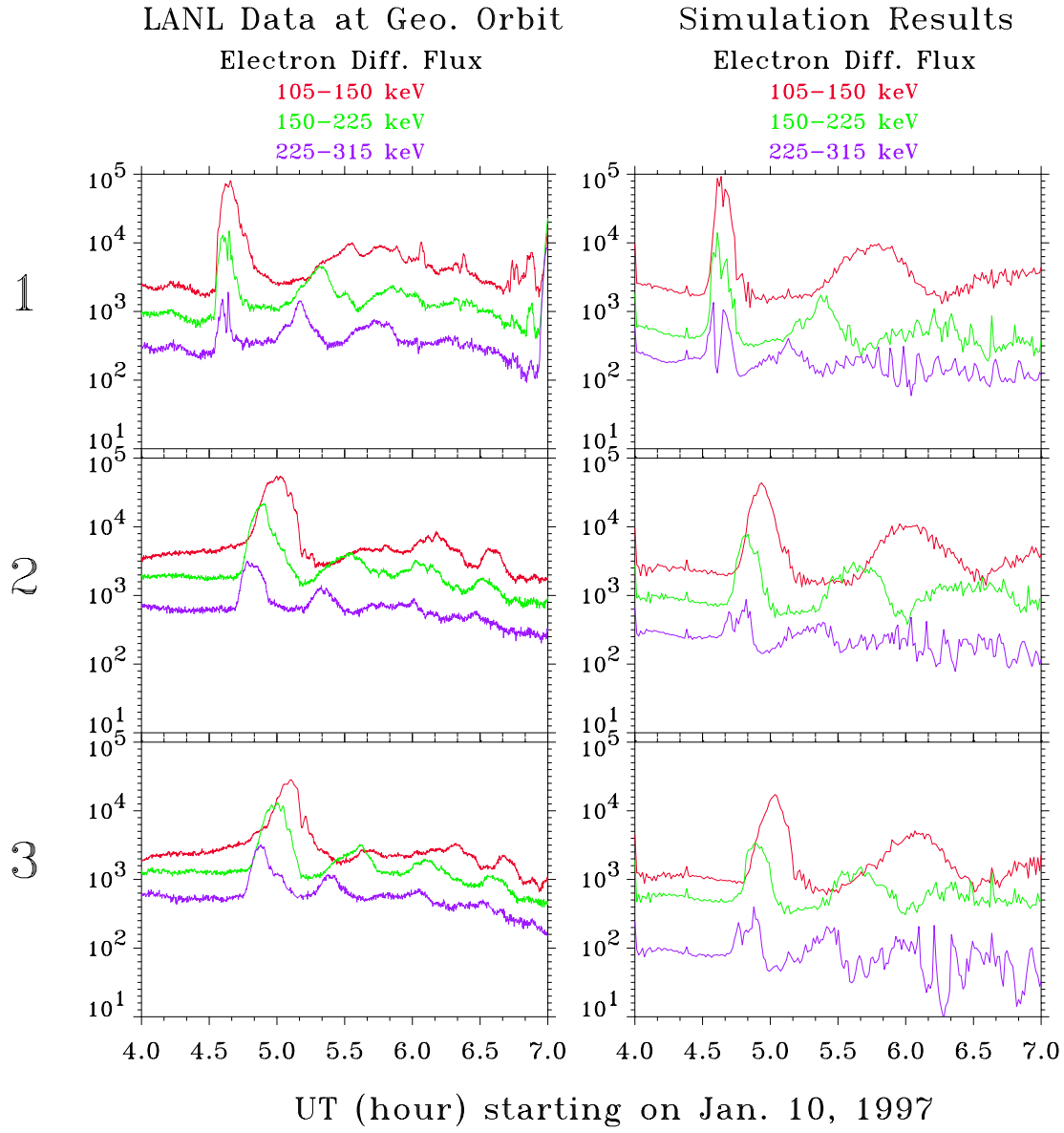

Figure 1

(Adapted from Figure 3 of Li et al., GRL, 1998)

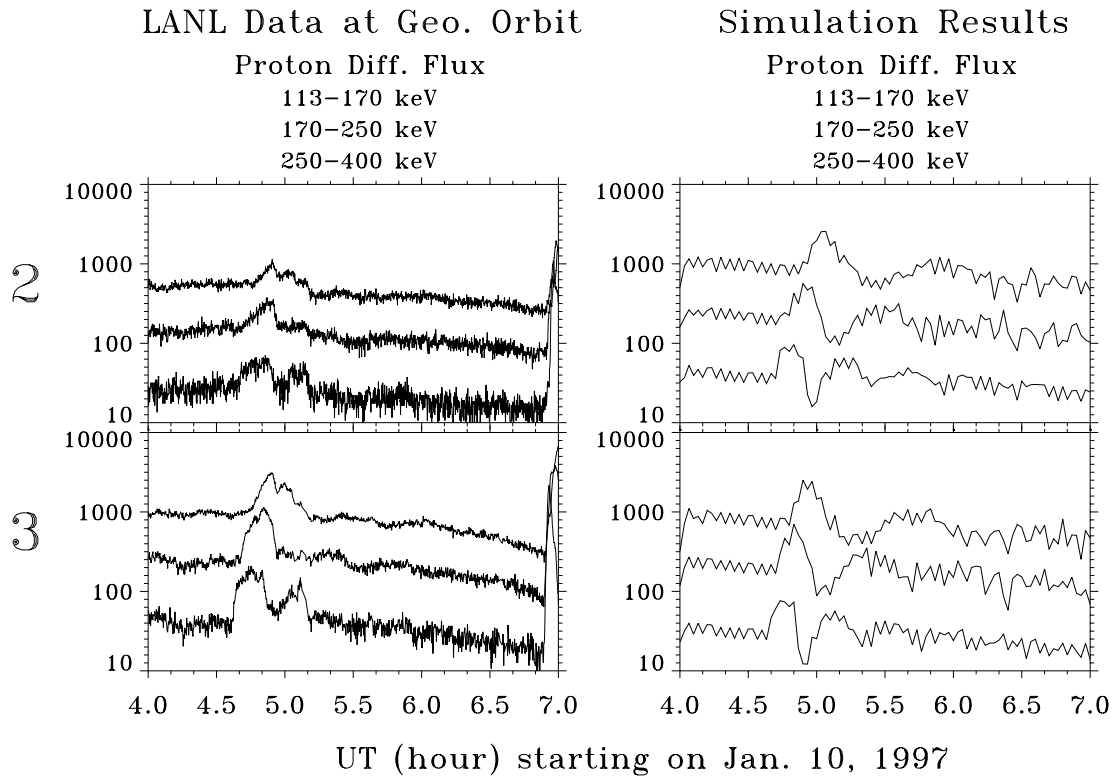
LANL Data at Geo. Orbit
Simulation Results
Proton Diff. Flux
113–170 keV
170–250 keV
250–400 keV
Proton Diff. Flux
113–170 keV
170–250 keV
250–400 keV
2
3
10000
1000
100
10
4.0
4.5
5.0
5.5
6.0
6.5
7.0
UT (hour) starting on Jan. 10, 1997

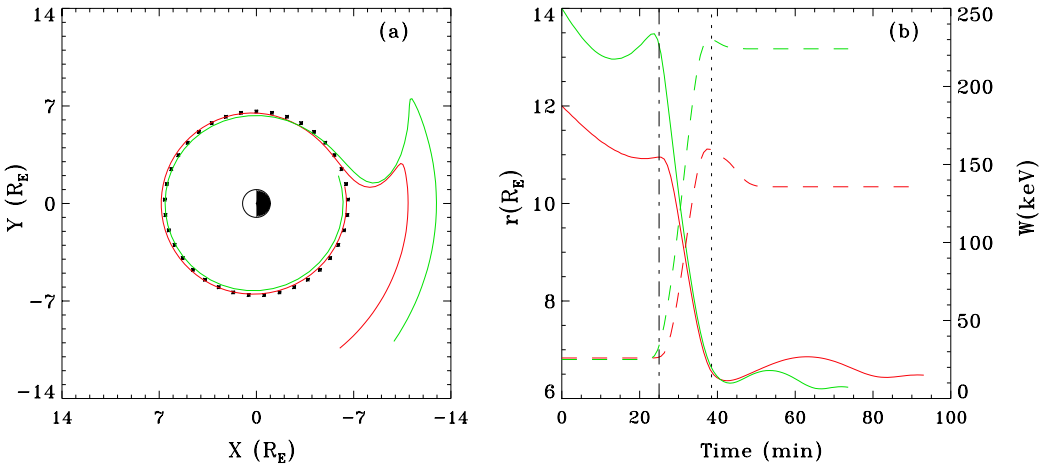
(a)
(b)
Y (R_E)
X (R_E)
r(R_E)
W(keV)
Time (min)
14
7
0
−7
−14
12
10
8
6
250
200
150
100
50
20
40
60
80
100

Figure 3